Anal. Chem. **2006,** *78,* 1418−1424

Scanning Electrochemical Microscopy Combined with Surface Plasmon Resonance: Studies of Localized Film Thickness Variations and Molecular Conformation Changes

Juan Xiang,[†] Jun Guo,[†] and Feimeng Zhou*[,‡]

Institute of Surface Analysis and Biosensing, College of Chemistry and Chemical Engineering, Central South University, Changsha 410083, P. R. China, and Department of Chemistry and Biochemistry, California State University, Los Angeles, California 90032

The combination of scanning electrochemical microscopy (SECM) with surface plasmon resonance (SPR) is described. By oxidizing ferrocenylalkanethiol self-assembled monolayer (SAM) with SECM-generated Ce^{4+}, the coupled technique, SECM-SPR, is shown to be viable for determining local variations in thin film thickness. Factors (tip/substrate distance, tip potential scan rate, and solution composition change) affecting the SECM-SPR response and operation are also discussed. The approach was further extended to the determination of conformational changes of cytochrome *c* molecules attached electrostatically onto a negatively charged SAM during its reduction by the tip-generated methyl viologen monocation. The high sensitivity of the SPR equipped with a bicell detector facilitates the measurement of infinitesimal film thickness changes accompanying redox reactions, while the SECM provides a means to obviate the necessity of applying a potential to the SPR substrate, which tends to cause unwanted interferences and complications. The approach also affords an avenue for determining film thickness variations that are not subject to certain effects, such as the surface charge, the heterogeneity of the substrate, and the distance between the redox center of the immobilized molecule and the underlying substrate electrode.

Since its inception, scanning electrochemical microscopy (SECM)[1−4] has been combined with a variety of analytical and surface techniques for studies of redox-induced surface reactions, investigation of properties of adsorbates, and evaluations of performances of select techniques.[5−15] The impetus behind developing these coupled techniques stems from the need for addressing interfacial phenomena with techniques that complement electrochemical means and the versatility and flexibility of using SECM tip electrodes to generate localized reactions and controllably create miniature surface patterns. Two approaches have been used to implement this coupling. The first approach, which involves positioning the SECM tip and cell directly above an instrument, is generally simpler in design and does not need significant modifications of the SECM or the instrument to be coupled. SECM-quartz crystal microbalance,[5,11,12] SECM-electrogenerated chemiluminescence,[6] and SECM-optical spectroscopy[7] are representative of this approach. The second approach requires the fabrication of novel SECM tips that accommodate simultaneous detections by both techniques. SECM-photelectrochemical spectroscopy,[16] SECM-atomic force microscopy,[9,13] electrochemical tunneling microscopy-SECM,[17] and SECM-microelectrode potentiometry,[8] to name a few, are hyphenated techniques developed with this approach. Though more complicated in tip construction, these techniques can yield remarkable spatial resolution and are typically more compact.

In recent years, surface plasmon resonance (SPR) has proved to be a highly sensitive technique for detecting adsorbates, especially biomacromolecular ones, at extremely low quantities.[18−27]

* Corresponding author. Phone: 323-343-2390. Fax: 323-343-6490. E-mail: fzhou@calstatela.edu.

[†] Central South University.

[‡] California State University, Los Angeles.

(1) Bard, A. J.; Mirkin, M. V. *Scanning Electrochemical Microscopy*; Marcel Dekker: New York, 2001.
(2) Bard, A. J.; Fan, F.-R. F.; Pierce, D. T.; Unwin, P. R.; Wipe, D. O.; Zhou, F. *Science* **1991**, *254*, 68−74.
(3) Mirkin, M. V. *Anal. Chem.* **1996**, 177A−182A.
(4) Engstrom, R. C.; Weber, M.; Wunder, D. J.; Burgess, R.; Winquist, S. *Anal. Chem.* **1986**, *58*, 844−848.
(5) Cliffel, D.; Bard, A. J. *Anal. Chem.* **1998**, *70*, 1993−1998.
(6) Fan, F.-R., F.; Cliffel, D.; Bard, A. J. *Anal. Chem.* **1998**, *70*, 2941−2948.
(7) Lee, Y.; Bard, A. J. *Anal. Chem.* **2002**, *74*, 3626−3633.
(8) Wei, C.; Bard, A. J.; Nagy, G.; Toth, K. *Anal. Chem.* **1995**, *67*, 1346−1356.
(9) Macpherson, J. V.; Unwin, P. R. *Anal. Chem.* **2000**, *72*, 276−285.
(10) Zhang, J.; Slevin, C. J.; Morton, C.; Scott, P.; Walton, D. J.; Unwin, P. R. *J. Phys. Chem. B* **2001**, *105*, 11120−11130.
(11) Hillier, A. C.; Ward, M. D. *Anal. Chem.* **1992**, *64*, 2539−2554.
(12) Gollas, B.; Bartlett, P. N.; Denault, G. *Anal. Chem.* **2000**, *72*, 349−356.
(13) Sklyar, O.; Kueng, A.; Kranz, C.; Mizaikoff, B.; Lugstein, A.; Bertagnolli, E.; Wittstock, G. *Anal. Chem.* **2005**, *77*, 764−771.
(14) Szunerits, S.; Knorr, N.; Calemczuk, R.; Livache, T. *Langmuir* **2004**, *20*, 9236−9241.
(15) Tsionsky, M.; Zhou, J.; Amemiya, S.; Fan, F.-R., F.; Bard, A. J. *Anal. Chem.* **1999**, *71*, 4300−4305.
(16) James, P.; Casilas, N.; Smyrl, W. H. *J. Electrochem. Soc.* **1996**, *143*, 3853−3865.
(17) Treutler, T. H.; Wittstock, G. *Electrochim. Acta* **2003**, *48*, 2923−2932.
(18) Piscevic, D.; Lawall, R.; Vieth, M.; Liley, M.; Okahata, Y.; Knoll, W. *Appl. Surf. Sci* **1995**, *90*, 425−436.
(19) Peterlinz, K. A.; Georgiadis, R.; Herne, T. M.; Tarlov, M. J. *J. Am. Chem. Soc.* **1997**, *119*, 3401−3402.
(20) Gotoh, M.; Hasegawa, Y.; Shinohara, Y.; Shimizu, M.; Tosu, M. *DNA Res.* **1995**, *2*, 285−293.

10.1021/ac051601h CCC: $33.50
Published on Web 02/03/2006

Because the SPR phenomenon is extremely sensitive to the refractive index of the medium (or solution composition) next to the metal film, adsorption of a trace amount of adsorbates at the surface or infinitesimal conformational/orientation changes in the adsorbed molecules can be detected. When combined with electrochemistry, the resultant coupled technique (EC-SPR) offers a viable avenue to probe optical and electronic properties of the adsorbates and provides a sensitive means to quantify thickness variations of ultrathin films accompanying redox reactions. Advincula, Knoll, and co-workers[28] and Kang et al.[29] used EC-SPR to investigate the electrochromic property of poly(3,4-ethylenedioxythiophene) and the electropolymerization of aniline, respectively. Boussaad et al. combined cyclic voltammetry with a multiwavelength SPR to determine conformational and electronic changes in redox proteins.[30] Recently, using a high-resolution SPR instrument capable of detecting SPR dip shifts as small as 1×10^{-5} deg,[31,32] we demonstrated that orientation changes of ferrocenyl alkanethiol self-assembled monolayers (SAMs), upon oxidation of the terminal ferrocene moieties, can be quantified.[33] Szunerits et al. used a ultramicroelectrode (UME) tip to generate micropatterns that can be simultaneously mapped by an imaging SPR.[14,34] In their work, the tip was merely used as a counter electrode to provide an electrical field for localized electropolymerization of pyrrole-labeled oligonucleotides at the substrate electrode. These approaches shed insight to the changes induced by an external field[35] or the transfer of electrons between the adsorbates and the underlying electrodes.[30,33] However, the external potential applied to the SPR substrate for a typical voltammetric experiment changes the substrate electron density and causes a SPR dip shift.[30,36] This inherent "interference" could become particularly problematic and must be excluded for cases where an extremely small thickness variation occurs.[30,33] Although one might expect that redox reactions could be induced by introducing a redox species into the solution, the drastic change in the solution composition (refractive index) would cause an even more pronounced interference. Thus, it will be highly desirable to initiate redox reactions without applying the potential to the SPR substrate or introducing a foreign redox species into the solution.

Herein, we report the combination of SPR with SECM to study localized thickness variation and conformational changes of adsorbate molecules. By using 6-ferrocenyl-1-hexanethiol SAM as a model system, we show that the aforementioned problem can be circumvented. Parameters important to the SECM-SPR operation are also investigated. The approach was then extended to the measurement of redox-induced conformational change of surface-immobilized cytochrome *c* (cyt *c*) molecules. We show that redox species launched from the small tip electrode induces a localized surface reaction or change at the substrate, affording an opportunity to examine thickness variation and related processes that might not be accurately measurable by conventional EC-SPR experiments. The open design of our SPR renders it amenable to combining SECM with SPR in a straightforward fashion, and the high sensitivity of the bicell detector for differential detection facilitates real-time detection of changes modulated by the tip-generated species.

EXPERIMENTAL SECTION

Chemicals and Materials. 6-Ferrocenyl-1-hexanethiol (FcC_6SH) was purchased from Dojindo Co. (Atlanta, GA). Cyt *c* was acquired from Sigma Chemical Co. (St. Louis, MO). Methyl viologen dichloride, hexanethiol, and 11-mercaptoundecanoic acid (MUA) were obtained from Aldrich (Milwaukee, WI). Nitric acid and $Ce(NO_3)_3$ (Beijing Reagent Co.) were of reagent grade and used as received. All solutions were prepared with deionized water (Milli-Q, Millipore Corp).

Instruments. *SPR.* The SPR setup is similar to what we have previously reported.[24,33] Briefly, a BK7 planocylindrical lens (Melles Griot, Carlsbad, CA) was used as the SPR prism. A BK7 glass slide (Fisher Scientific, Tustin, CA), coated with a 50-nm-thick gold film and a 2-nm Cr underlayer using a sputter coater (Cressington model 108SE, Ted Pella, Inc. Redding, CA), was placed onto the prism with an index-matching fluid (Cargille Laboratories, Cedar Grove, NJ). A diode laser with emission wavelength at 785 nm was controlled by a LDC 500 laser driver (Thorlabs, Newton, NJ). Our SPR instrument measures light reflected onto the two photodetectors of a bicell detector (A and B, cf. Figure 1) and the SPR dip shift is proportional to the ratio of $(A - B)/(A + B)$.[31] The lens placed between the laser diode and the SPR prism help focus the laser beam into a fine spot with variable diameters. We found that a spot with a diameter of ~100 μm yielded the highest SPR sensitivity. The SPR signals were recorded via a data acquisition board (PCI-1731, Advantech Co., Inc.) controlled by a Labview program. Conversion of the $(A - B)/(A + B)$ values to SPR angle changes follows our previously published procedure.[37]

SECM. A beveled 10-μm-diameter Au UME tip with a RG[1,38] of about 8−10 was mounted onto a SECM (CHI900B, CH Instruments, Austin, TX). A Ag/AgCl and a Pt wire served as the reference and auxiliary electrodes, respectively.

Procedures. *SPR Substrate Preparations.* The gold-coated glass slide was annealed in a hydrogen flame to eliminate surface contamination. Upon soaking the slide in a hexane solution

(21) Sawata, S.; Kai, E.; Ikebukuro, K.; Iida, T.; Honda, T.; Karube, I. *Biosens. Bioelectron.* **1999**, *14*, 397−404.
(22) Nelson, B. P.; Grimsrud, T. E.; Liles, M. R.; Goodman, R. M.; Corn, R. M. *Anal. Chem.* **2001**, *73*, 1−7.
(23) He, L.; Musick, M. D.; Nicewarner, S. R.; Salinas, F. G.; Benkovic, S. J.; Natan, M. J.; Keating, C. D. *J. Am. Chem. Soc.* **2000**, *122*, 9071−9077.
(24) Song, F.; Zhou, F.; Wang, J.; Tao, N.; Lin, J.; Vellanoweth, R.; Morquecho, Y.; Wheeler-Laidman, J. *Nucleic Acids Res.* **2002**, *30*, e72/1−e72/11.
(25) Giakoumaki, E.; Minunni, M.; Tombelli, S.; Tothill, I. E.; Mascini, M.; Bogani, P.; Buiatti, M. *Biosens. Bioelectron.* **2003**, *19*, 337−344.
(26) Goodrich, T. T.; Lee, H. J.; Corn, R. M. *J. Am. Chem. Soc.* **2004**, *126*, 4086−4087.
(27) Wang, Q.; Wang, J.-F.; Geil, P. H.; Padua, G. W. *Biomacromolecules* **2004**, *5*, 1356−1361.
(28) Baba, A.; Lubben, J.; Tamada, K.; Knoll, W. *Langmuir* **2003**, *19*, 9058−9064.
(29) Kang, X.; Jin, Y.; Cheng, G.; Dong, S. *Langmuir* **2002**, *18*, 1713−1718.
(30) Boussaad, S.; Pean, J.; Tao, N. J. *Anal. Chem.* **2000**, *72*, 222−226.
(31) Tao, N. J.; Boussaad, S.; Huang, W. L.; Arechabaleta, R. A.; D'Agnese, J. *Rev. Sci. Instrum.* **1999**, *70*, 4656−4660.
(32) Wang, S.; Boussaad, S.; Tao, N. J. *Anal. Chem.* **2000**, *72*, 4003−4008.
(33) Yao, X.; Wang, J.; Zhou, F.; Wang, J.; Tao, N. *J. Phys. Chem. B* **2004**, *108*, 7206−7212.
(34) Frotin, E.; Defontaine, Y.; Mailley, P.; Livache, T.; Sczunerits, S. *Electroanalysis* **2005**, *17*, 495−503.
(35) Hanken, D. G.; Corn, R. M. *Anal. Chem.* **1997**, *69*, 3665−3673.
(36) Kittle, C. *Solid State Physics*; John Wiley & Sons: New York, 1996.
(37) Kolomenskii, A. A.; Gershon, P. D.; Schuessler, H. A. *Appl. Opt.* **1997**, *36*, 6539−6547.
(38) Kwak, J.; Bard, A. J. *Anal. Chem.* **1989**, *61*, 1221−1227.

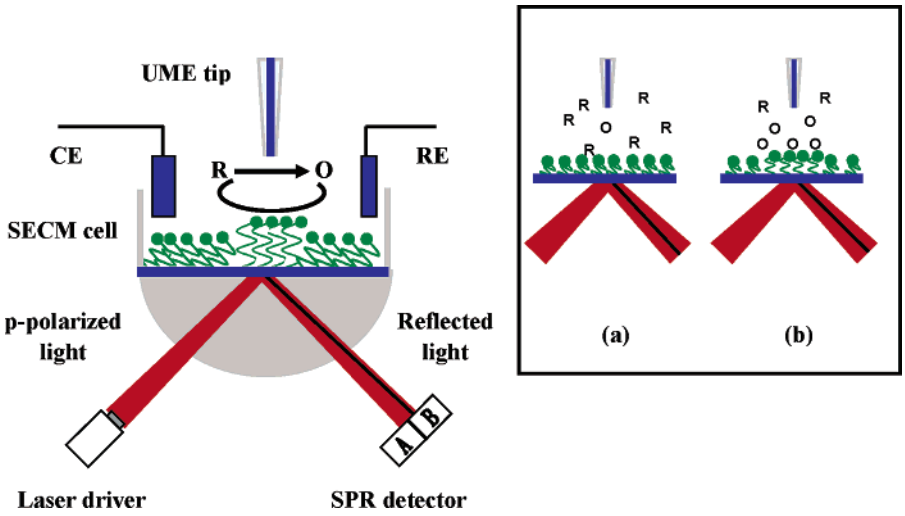

Figure 1. SECM-SPR combination for studies of redox-induced, localized film thickness variation and molecular orientation changes. Oxidation of redox moieties at the film by a tip-generated oxidant (O) is used as an example. The SECM cell containing the counter electrode (CE), the reference electrode (RE), and the UME tip is mounted directly onto of the SPR prism and instrument. Inset: schematic representations of the diffusion zones at the moment when O is generated at the tip (a) and at the time when O is produced at the diffusion-controlled rate (b). Notice that the area illuminated by the laser spot is much greater than the tip size and the position of the SPR dip (dark line) has changed from (a) to (b) upon the molecular orientation change.

containing 1.0 mM FcC_6SH for 12 h, the surface was rinsed liberally with hexane and water. For the cyt *c* film formation, a MUA SAM was first attached to the surface by immersing the gold film in 2.0 mM MUA for 12 h. The MUA-covered film was then submerged in a 50 mM phosphate buffer (pH 7.0) containing 0.5 mM cyt *c* for 20 min.

SECM-SPR Measurements. The SPR substrate covered with a film of interest was mounted onto the prism holder and the Teflon cell.[33] With the cell empty and the film normal to the UME tip, the UME tip was moved horizontally over the small laser spot refracted from the back of the gold film. Positioning the tip closer to the substrate surface can be accomplished by monitoring the feedback current of 1.0 mM $K_3Fe(CN)_6$ in a 0.1 M KCl solution. Upon reaching the desired tip/substrate distance (*d*), the $K_3Fe(CN)_6$ solution was pipetted out and the cell was washed and refilled with the solution to be used for the subsequent SECM-SPR experiments.

RESULTS AND DISCUSSION

Figure 1 illustrates the principle behind the SECM-SPR combination for sensitive measurements of film thickness variation and orientation changes of surface-confined molecules in a highly localized area. At a close *d*, an oxidant (reductant) electrogenerated at the UME tip rapidly diffuses to the SPR substrate and oxidizes (reduces) the molecules affixed onto the surface. The redox reaction induces an infinitesimal change of the ultrathin film. These changes result in a shift of the SPR dip, which can be sensitively detected by the bicell detector.[24,30,33] Because the UME tip is smaller than the laser spot impinging onto the back of the SPR substrate, the magnitude of the SPR dip shift is dependent on the amount of tip-generated species that will reach the substrate. If the tip potential were scanned fast and the tip/substrate distance were relatively large, the change of the SPR dip position would be small.

We first studied the redox-induced thickness variation of ferrocenylalkanethiol SAMs to establish this coupled method. The following reactions take place at the UME tip and the $Fc-C_6SH$ SAM.

$$\text{SECM tip:} \quad Ce^{3+} - e^- \rightarrow Ce^{4+} \qquad (1)$$

SPR substrate:

$$Ce^{4+} + FcC_6S-Au \rightarrow Ce^{3+} + Fc^+C_6S-Au \qquad (2)$$

Ce^{4+}, produced from electrochemical oxidation of 0.01 M $Ce(NO_3)_3$ in a 0.1 M HNO_3 solution (reaction 1), participates in an electron-transfer (ET) reaction with $Fc-C_6SH$ SAM at the substrate (reaction 2). A similar reaction, with electrogenerated $Ru(bpy)_3^{3+}$ as the oxidizer, was used by Unwin and co-workers to probe the charge propagation of a *N*-octadecylferrocenecarboxamide film at the water/air interface.[10] Ce^{3+} regenerated in reaction 2 increases the UME tip current (SECM positive feedback). At the same time, the thickness of the $Fc-C_6SH$ SAM oxidized underneath the tip becomes greater than the surrounding areas, due to the electrostatic repulsion among the ferrocenium ions.[39] Figure 2 shows a linear scan voltammogram of Ce^{3+} (a, curve 1) and the simultaneously recorded SPR dip shift-time diagram of FcC_6SH SAM (b, curve 1) at $d = 9$ μm. Responses from two control experiments are also shown. In the first control, the voltammogram and the corresponding SPR response acquired in the absence of Ce^{3+} are shown as curves 2 in Figure 2a and b, respectively. In the second control, Ce^{4+} generated at the UME tip was allowed to diffuse to a SPR substrate covered with a hexanethiol SAM (curves 3 in Figure 2a and b).

Generation of Ce^{4+} occurs at the onset of the voltammogram (at ~1.22 V or ~62 s after the potential scan was initiated). Based on the relation $t = d^2/D$ (where *D* is the diffusion coefficient of Ce^{3+}),[40−42] the time (*t*) for Ce^{4+} to diffuse from the tip to the SPR substrate and across the area on the substrate covered by the laser spot can be estimated. Using the diffusion coefficient 1.8 ×

(39) Ye, S.; Sato, Y.; Uosaki, K. *Langmuir* **1997**, *13*, 3157−3161.

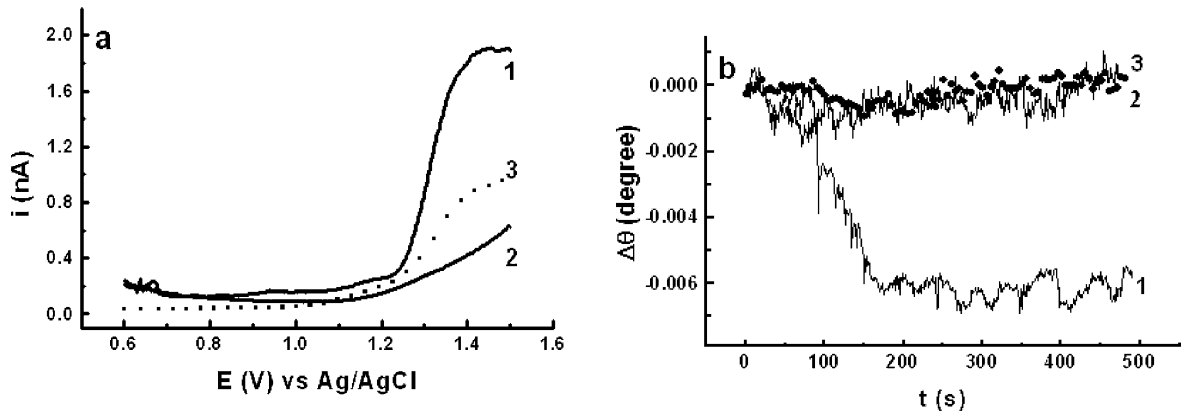

Figure 2. Linear scan voltammogram of 0.01 M $Ce(NO_3)_3$ at a Au UME tip (a, curve 1) and the corresponding SPR dip shift-time diagram of FcC_6SH SAM (b, curve 1). The same measurements were conducted in a HNO_3 solution without $Ce(NO_3)_3$ (curves 2 in both panels). The voltammogram and the SPR dip-time diagram acquired in a 0.01 M $Ce(NO_3)_3$ solution at a SPR substrate covered with a hexanethiol SAM are shown as dotted curves 3 in (a) and (b). The tip/substrate distance for all the experiments was ~9 μm and the potential scan rate was 10 mV/s.

10^{-6} cm^2/s estimated from chronoamperometry at a UME electrode,[43] the time for Ce^{4+} to travel across the tip/substrate gap ($d = 9$ μm) was deduced to be 0.47 s and that to traverse across the area covered by the laser spot (radius ~50 μm) to be 14.5 s, respectively. Thus, Ce^{4+}, upon generation, can rapidly reach the surface directly underneath the UME tip. However, the development of the diffusion zone fully encompassing the area of the substrate covered by the laser spot (cf. Figure 1) takes a much longer time. Notice in Figure 2b, only at ~13 s after the Ce^{4+} generation (i.e., 75 s) did the SPR dip begin to change. Such a time is in good agreement with the duration we estimated for Ce^{4+} to diffuse across the spot covered by the laser beam. Therefore, it is evident that the amount of Ce^{4+} initially arriving at the surface was not sufficient to create an appreciable SPR dip shift. After the Ce^{4+} flux electrogenerated at the diffusion-controlled rate has fully diffused across the laser spot, the SPR began to sense an appreciable change of the film thickness. Notice that the net change in curve 1, 0.0065°, is quite small and would be difficult to measure by a less sensitive SPR instrument.

Interestingly, a closer examination of the time lapse and the shape of the FcC_6SH SPR response in the Ce^{3+} solution reveals that the completion of the potential scan (1.5 V or 90 s after the scan initiation in panel a) does not coincide with the time when the steady-state SPR dip value is attained (150 s in panel b). This suggests that the film was still undergoing reorganization even after the potential scan had been finished. It seems that the localized FcC_6SH SAM thickness variation induced by the tip-generated oxidant might be slower than that resulting from oxidizing the entire FcC_6SH SAM in the conventional EC-SPR configuration.[33] It is conceivable that FcC_6SH molecules surrounding those that have been oxidized by Ce^{4+} could impose an impediment of the film reorientation, causing the delay in the SPR dip shift.

The fact that curve 1 in Figure 2b remains at the steady-state value more than 400 s after the termination of the potential scan (cessation of the electrogeneration of Ce^{4+}) suggests that the change in the film thickness is irreversible. This observation indicates that the lateral propagation of charges on the ferrocenium entities is slow on the time scale of the SECM-SPR studies. Moreover, tunneling of the charges across the alkanethiol chain or through the space occupied by the $Fc-C_6SH$ SAM is also negligible when no potential bias is applied to the substrate. We conducted a separate experiment in an attempt to confirm the "charge confinement" in the localized SAM by recording the feedback current at the UME tip during multiple scans within the potential range shown in Figure 2a. We found that the steady-state current decreased from a positive feedback current during the first scan (e.g., 1.8 nA at $d = 9$ μm) to a negative one during the second scan (0.83 nA, which is smaller than $i_{T,\infty} = 1.3$ nA), and the negative feedback remained unchanged for at least 600 s.

In contrast to the sigmoidal SPR dip-time diagram (curve 1 of Figure 2b), the SPR signal collected in the absence of Ce^{3+} changed little, except in two regimes where tiny fluctuations occurred (0.001° within 0−60 s and 0.0009° within 410−500 s in curve 2 of Figure 2b). The small fluctuation in regime 1 can be attributed to the minor change in the refractive index of the solution, caused largely by the rapid oxidation of the electrolyte solution at an extreme potential (cf. the rising portion of curve 2 of Figure 2a). After the potential scan, the solution composition within the tip/substrate gap gradually recovered to that of the bulk solution and consequently the SPR dip returned to the original value (regime 2). Curve 3 in Figure 2a, which is a voltammogram collected at a UME tip over a hexanethiol SAM, shows a SECM negative feedback ($i_{T,\infty} = 1.3$ nA), indicating that Ce^{4+} cannot be reduced without ferrocene groups present at the substrate. The simultaneously recorded SPR dip-time diagram (curve 3 in Figure 2b) suggests that the thickness of a hexanethiol SAM was essentially unperturbed by the tip-generated Ce^{4+}. Thus, the conversion of a SECM mediator between its redox states is more advantageous than the introduction of a redox species of a relatively high concentration into the sample solution, since the refractive index of the solution confined within the tip/substrate gap in the former approach is not changed appreciably. We also ruled out the possible effect of temperature variation given rise by the passage of the faradaic current on the solution refractive

(40) Zhou, F.; Unwin, P. R.; Bard, A. J. *J. Phys. Chem.* **1992**, *96*, 4917−4924.
(41) Kiekens, P.; Steen, L.; Donche, H.; Temmerman, E. *Electrochim. Acta* **1981**, *26*, 841−845.
(42) Bard, A. J.; Faulkner, L. R. *Electrochemical Methods. Fundamentals and Applications*; John Wiley & Sons: New York, 2001.
(43) Denault, G.; Mirkin, M. V.; Bard, A. J. *J. Electroanal. Chem* **1991**, *308*, 27−38.

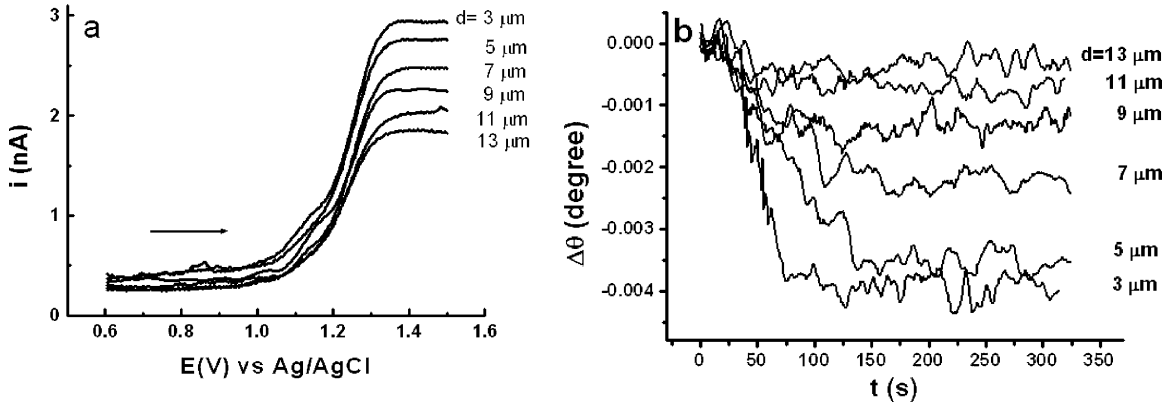

Figure 3. Linear scan voltammograms of 0.01 M $Ce(NO_3)_3$ (a) in a 0.1 M HNO_3 solution at different tip/substrate distances and the simultaneous SPR dip shift curves of the FcC_6SH SAM (b). The exact tip/substrate distances are shown next to the curves. The scan rate was 30 mV/s. The arrow in (a) indicates the potential scan direction.

index change. For current as small as 1−2 nA, and the small volume of solution confined within a tip/substrate gap of 9 μm, the temperature variation was deduced to be about $(1.5-3.0) \times 10^{-7}$ K. Such a tiny temperature change would cause a change of refractive index of the solution by $(1.8-3.6) \times 10^{-11}$,[44] which is several orders of magnitude lower than the detection limit of our instrument.[24] The SPR dip shift that might be affected by the influx of the counteranions needed to balance the positive charges on the ferrocenium moieties also should not be significant. As discussed in our previous work,[33] the refractive index of a relatively dilute HNO_3 solution (e.g., $n = 1.3328$ for a 0.1 M HNO_3 solution) does not deviate much from that of water ($n = 1.33$). As a result, a five-phase Fresnel calculation that includes the layer of NO_3^- with the refractive index measured from 0.1 M HNO_3 yielded a dip shift of only 0.0004°.[33] This is more than 1 order of magnitude smaller than the dip shift in curve 1 of Figure 2b. Furthermore, if the $Fc-C_6SH$ SAM is assumed to be of the hexagonal close packing,[45] the increase of NO_3^- ions next to the $Fc-C_6SH$ SAM will only be ~0.84 μM. Thus, the refractive index of this liquid layer would be even closer to that of water, and we conclude the anionic layer situated on top of the ferrocenium SAM can be considered as a continuum of the electrolyte solution. Perhaps one of the more important processes that could contribute to the observed SPR dip shift is water loading associated with the ion pairing process. Previously, we have shown that hydration of NO_3^- could bring water molecules onto or into oxidized ferrocenylalkanethiol SAM[33] and subsequently change the refractive index of film. Under the extreme condition (assuming no water molecules present in the ferrocenylalkanethiol film and all the void space in the film would be occupied by water upon the film oxidation[33]), the contribution could be as high as 50% of the total SPR dip shift. In reality, for an anion with a relatively small effective hydrated radius (e.g., NO_3^-),[46] the contribution from water loading should be much less.

We also studied the effect of d on the SPR signal. As in the discussion of curve 1 of Figure 2a, when the flux of the tip-generated Ce^{4+} is large and the area covered by the laser spot (~100 μm in diameter) is small, the extent of the SPR dip shift is not strongly dependent on the distance. This suggests that most of the FcC_6SH molecules covered by the laser spot have been oxidized by the tip-generated Ce^{4+}. In an attempt to observe a more pronounced effect, we reduced the Ce^{4+} flux by increasing the scan rate to 30 mV/s. The tip current increased inversely with d (Figure 3a). We should note that each set of curves was obtained at a different portion of the same film. Studying different areas of a film can be conveniently performed by sliding the SECM/SPR cell in the direction that is normal to the plane of incidence (cf. Figure 1). The SECM positive feedback suggests that Ce^{4+} reaching (or "collected by") the SPR substrate has been reduced back to Ce^{3+} (see also reaction 2). The same reaction causes the oxidation of the Fc groups and the subsequent thickness variation (Figure 3b). Analogous to the substrate current in the SECM tip generation/substrate collection (TG/SC) mode,[40,47,48] the SPR dip shift increases as d decreases. In the conventional SECM TG/SC mode,[40,47,48] the substrate can continuously drain out/transfer in electrons and serves as a "renewable" collector. An unit collection efficiency can be achieved at a distance equal to or shorter than the tip radius.[40,49] In the SECM-SPR configuration, if the area of the film covered by the SPR laser spot has undergone complete thickness change, the SPR substrate will no longer be responsive to additional flux of the tip-generated species. Thus, the SPR substrate "collection efficiency" depends not only on d but also on other parameters, such as the surface density of the immobilized molecules, the area covered by the SPR laser spot, and the tip potential scan rate.

As mentioned in the introduction, in the conventional EC-SPR approach, ET occurs between the substrate electrode and surface adsorbates. The application of a potential (ΔV) to the metal film electrode will cause a change in its electron density (Δn_e), which in turn will result in a variation of the dielectric constant ($\Delta\epsilon_m$). Δn_e is given by

$$\Delta n_e = -(C_{dl}\Delta V)/ed_m \quad (3)$$

where C_{dl} is the double layer capacitance, e is the electronic charge (-1.602×10^{-19} C), and d_m is the thickness of the metal film.[50]

(44) Chiang, H.-P.; Wang, Y.-C.; Leung, P. T. *Thin Solid Films* **2003**, *425*, 135−138.
(45) Widrig, C. A.; Alves, C. A.; Porter, M. D. *J. Am. Chem. Soc.* **1991**, *113*, 2805−2810.
(46) Kielland, J. *J. Am. Chem. Soc.* **1937**, *59*, 1675−1678.

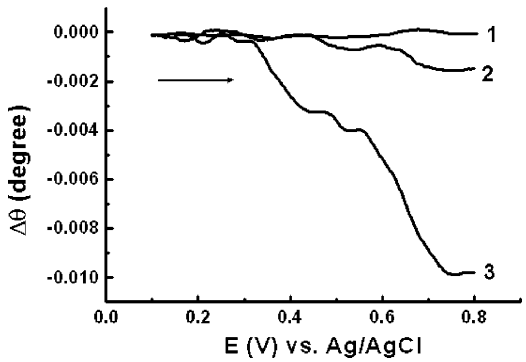

Figure 4. SPR dip shift-potential diagrams collected with SECM-SPR (curve 1) and the conventional EC-SPR approach (curves 2 and 3). For curve 1, the tip was positioned 9 μm over a HT-SAM immersed in a 0.01 M $Ce(NO_3)_3$/0.1 M HNO_3 solution. Curve 2 was obtained at a HT-SAM, whereas curve 3 was acquired at a FcC_6SH SAM-covered substrate submerged in a 0.1 M HNO_3 solution. The scan rate for all cases was 30 mV/s. The arrow indicates the potential scan direction.

$\Delta\epsilon_m$ is related to Δn_e as follows,

$$\Delta\epsilon_m = (\epsilon_m - 1)(\Delta n_e/n_e) \quad (4)$$

where ϵ_m and n_e are the dielectric constant and electron density of a metal film, respectively.[50] If C_{dl} of an adsorbate-covered metal film[42] is assumed to be 2 μF/cm^2, and $\epsilon_m = -11.8$, $n_e = 5.85 \times 10^{22}$/cm^2, and $d_m = 50$ nm, applying 1 V to the substrate electrode would lead to a change of $\Delta\epsilon_m$ of 0.0002[50] or an angular shift by 0.002°. Such a value would be a significant fraction of the small SPR signal shown in curve 1 of Figure 2b. Thus, circumventing ET between the substrate and the Fc groups via the SECM-SPR approach should eliminate the effect of an applied potential on the variation of the electron density in the SPR substrate. A comparison of the SPR dip shift-potential diagrams collected at two hexanethiol SAM-modified SPR substrates (curves 1 and 2 in Figure 4) illustrates this point. While curve 1 (SECM-SPR) remained unchanged, the net SPR dip shift in curve 2 (EC-SPR) is about ~0.0016°. We chose this potential range because it was used in our previous EC-SPR measurements of ferrocenylalkane SAMs.[33] A representative EC-SPR curve (curve 3) acquired at a Fc−C_6SH SAM showed a total dip shift by 0.010°. Thus, the effect of a potential scan at the substrate caused an "interference" whose magnitude is 16% of the analytical signal. We should add that the surface structure of the hexanethiol SAM is also different from that of the FcC_6SH SAM.[33] In other words, the alkanethiol SAM generally used for the background correction[30,33] does not unambiguously mimic the structure of the FcC_6SH SAM-modified surface.

The absence of an externally applied potential to the substrate also excludes the electrostatic repulsion between the positively biased gold surface and the ferrocenium ions.[51,52] At the potential where Fc groups are oxidized, the applied potential is known to be more positive than the point of zero charge of a SAM-modified gold surface.[53] Consequently, the positively polarized electrode surface can also expel the Fc^+ ions, providing another driving force for the film thickness increase.[51,52] In fact, the SPR dip shift associated with FcC_6SH SAM oxidation measured by EC-SPR (~0.01° in curve 3 of Figure 4), even after background correction (~0.084°), is still markedly greater than that deduced from the SECM-SPR value (~0.0065° from Figure 2b). Thus, not only is the SPR dip shift measured by SECM-SPR more reliable but it is also more closely correlated with the film thickness variation initiated by the repulsion among the adjacent ferrocenium ions.

Finally, we extended the SECM-SPR approach to the study of redox-induced conformational changes of immobilized cyt *c* molecules. Cyt *c* is a well-studied redox protein[54] whose conformations are suggested to be dependent on its redox states.[55−57] However, the conformational changes measured by small-angle X-ray scattering measurements,[55] NMR spectroscopy,[56] and X-ray crystallography[57] vary over a relatively wide range (e.g., from 0.18 [55] to 0.38 Å [57]). Recently, Boussaad et al. measured redox-triggered conformational changes of cyt *c* using a high-resolution multiwavelength EC-SPR and obtained a change of ~0.5 Å.[30] It is generally believed that the protein conformations are also dependent on other factors such as solvation and ionic strength.

In our SECM-SPR approach, cyt *c* molecules are electrostatically adsorbed onto the negatively charged MUA SAM at the SPR gold substrate. Methyl viologen monocations (MV^+), generated at the tip from MV^{2+}, served as the reductant to convert the oxidized state of cyt *c* molecules (cyt c^+) to the reduced state (cyt c^0):[58]

$$\text{SECM tip:} \quad MV^{2+} + e^- \rightarrow MV^+ \quad (5)$$

$$\text{SPR substrate:} \quad MV^+ + \text{cyt } c^+ \rightarrow MV^{2+} + \text{cyt } c^0 \quad (6)$$

Reaction 6 reduces cyt c^+ and regenerates MV^{2+}, leading to SECM positive feedback. This reaction resulted in a net SPR dip shift by ~0.004° (curve 1 in Figure 5b). Such a dip shift corresponds to an increase of 0.27 ± 0.03 Å (number of replicates, 3). In deducing the conformation change, we used the Lorentz−Lorenz relation to calculate the relationship between the refractive index of cyt *c* film and the film thickness and performed a Fresnel calculation to relate the dip shift to the cumulative thickness change.[30,36] While this change is smaller than the value gauged by the EC-SPR,[30] it is well within those measured by small-angle X-ray scattering[55] and X-ray crystallography.[57] As aforementioned, the EC-SPR measurements are subject to uncertainties caused by the dependence of SPR dip shift on the applied potential. As a result, the background change needs to be subtracted from the overall SPR

(47) Treichel, D. A.; Mirkin, M. V.; Bard, A. J. *J. Phys. Chem.* **1994**, *98*, 5751−5757.
(48) Engstrom, R. C.; Meaney, T.; Tople, R.; Wightman, R. M. *Anal. Chem.* **1987**, *59*, 2005−2010.
(49) Lee, C.; Kwak, J.; Anson, F. C. *Anal. Chem.* **1991**, *63*, 1501−1504.
(50) Wang, S.; Boussaad, S.; Tao, N. J. In *Surfactant Science Series*; Rusling, J. F., Ed.; Marcel Dekker: New York, 2003; Vol. 111, pp 213−251.
(51) Uosaki, K.; Sato, Y.; Kita, H. *Langmuir* **1991**, *7*, 1511−1514.
(52) Uosoki, K.; Sato, Y.; Kita, H. *Electrochim. Acta* **1991**, *36*, 1793−1798.
(53) Creager, S. E.; Rowe, G. K. *J. Electroanal. Chem* **1997**, *420*, 291−299.
(54) Scott, R. A.; Mauk, A. G. *Cytochrome c. A Multidisciplinary Approach*; University Science Books: Sausalito, CA, 1995.
(55) Trewhella, J.; Carlson, V. A. P.; Curtis, E. H.; Heidorn, D. B. *Biochemistry* **1988**, *27*, 1121−1125.
(56) Feng, Y.; Roder, H.; Englander, S. W. *Biochemistry* **1990**, *29*, 3494−3504.
(57) Berghuis, A. M.; Brayer, G. D. *J. Mol. Biol.* **1992**, *223*, 959−976.
(58) Ferreyra, N. F.; Dassie, S. A.; Solis, V. M. *J. Electroanal. Chem* **2000**, *486*, 126−132.

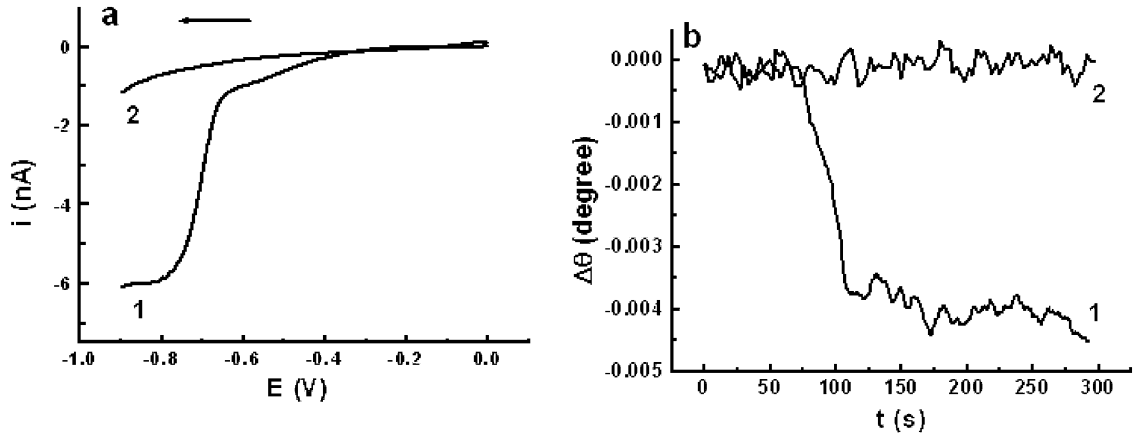

Figure 5. Linear scan voltammogram of 2.5 mM MV^{2+} in a 0.05 M phosphate solution (curve 1, a) and the simultaneous SPR dip shift-time diagram of cyt *c* attached on top of the MUA SAM at the SPR substrate (curve 1, b). Curves 2 in (a) and (b) correspond to the voltammogram at the SECM tip in a 0.05 M phosphate solution without MV^{2+} and the simultaneous SPR dip shift-time diagram, respectively. The distance between the tip and the substrate was ~9 μm, and the scan rate was 10 mV/s. The arrow indicates the scan direction.

dip shift.[30,33] Again as shown by curve 2 in Figure 5b, scanning the tip potential does not affect the SPR signal at the substrate. Another potential advantage of the SECM-SPR approach is that the ET process, occurring between a solution species in the tip/substrate gap and the redox termini on the film (which are largely exposed to solution), should be more effective than that between the electrode and the redox termini through spacer molecules. In the latter case, the electron-transfer rate can be much attenuated by unfavorable orientations of the redox centers with respect to the electrode,[59] the length and structure of the spacer molecule,[60] and the heterogeneity of the substrate electrode.

CONCLUSION

The simple and open design of the SPR instrument equipped with a bicell detector is well suited for the SECM-SPR combination. Using SECM-SPR, we have shown that small changes of film thickness and molecular orientations can be electrochemically induced and sensitively detected by SPR. By applying this coupled technique to studies of the redox-induced ferrocenylalkanethiol SAM thickness variation and cytochrome *c* conformational change, we evaluated experimental parameters affecting the SPR responses (i.e., tip/substrate distance, tip potential scan rate, and solution composition). Compared to conventional EC-SPR, the major advantage associated with this combination is that the change of electron density or the SPR dip shift caused by the potential applied to or scanned at the SPR substrate is eliminated. Consequently, thickness measurements by SPR become more reliable. The SECM also provides the flexibility of creating a localized surface change that cannot be achieved by directly applying the potential to the substrate. Therefore, complications resulted from other surface-related parameters (e.g., charges at the substrate surface, electron-transfer through the space and the bonds of a spacer molecule, and orientation of the immobilized molecules) can be avoided.

ACKNOWLEDGMENT

Partial support of this work by the National Natural Science Foundation of China (20225517 and 20503040), the Cultivation Fund of the Ministry of Education of China (704036), and a NIH-SCORE subproject (GM 80101) is gratefully acknowledged. We also thank Drs. F. Song and J. Wang for their technical assistance.

Received for review September 7, 2005. Accepted December 30, 2005.

AC051601H

(59) Murgida, D. H.; Hildebrandt, P. *J. Mol. Struct.* **2001**, *565−566*, 97−100.
(60) Murgida, D. H.; Hildebrandt, P. *Acc. Chem. Res.* **2004**, *37*, 854−861.